Atmospheric Research 114–115 (2012) 1–16

Contents lists available at SciVerse ScienceDirect

Atmospheric Research

journal homepage: www.elsevier.com/locate/atmos

Recovering of the energy spectra of electrons and gamma rays coming from the thunderclouds

Ashot Chilingarian, Bagrat Mailyan *, Levon Vanyan

A. Alikhanyan National Laboratory, Yerevan Physics Institute, Alikhanyan Brothers 2, Yerevan, Armenia

ARTICLE INFO

Article history:
Received 9 October 2011
Received in revised form 25 April 2012
Accepted 11 May 2012
Available online 19 May 2012

Keywords:
Thunderclouds
Atmospheric electricity
Lightning

ABSTRACT

Strong electric fields inside thunderclouds give rise to enhanced fluxes of high-energy electrons and, consequently, gamma rays and neutrons. During thunderstorms at Mount Aragats, hundreds of Thunderstorm Ground Enhancements (TGEs) comprising millions of energetic electrons and gamma rays, as well as neutrons, were detected at Aragats Space Environmental Center (ASEC) on 3200 m altitude. Observed large TGE events allow for the first time to measure the energy spectra of electrons and gamma rays well above the cosmic ray background. The energy spectra of the electrons have an exponential shape and extend up to 30–40 MeV. Recovered energy spectra of the gamma rays are also exponential in energy range 5–10 MeV, then turns to power law and extends up to 100 MeV.

1. Introduction: Thunderstorm ground enhancements (TGEs)

The attempts to discover high-energy phenomena in the atmosphere, so called, Thunderstorm Ground Enhancement (TGE), in spite of a long history since prediction of C.R.T. Wilson in 1924 (Wilson, 1925), were discrepant and rare. Early measurements (Schonland, 1930; Schonland and Viljoen, 1933) reported the existence of electron flux simultaneously, or earlier, than lightning located 30 km apart. Atop Mount Lemmon (altitude 2800 m) at the lightning research facility of the University of Arizona, the simultaneous detection of cosmic ray flux (by the 10-cm diameter and 10-cm length plastic scintillator) and electric field (by an electric field mill) demonstrates ~10% enhancement of the 1-minute count (Shaw, 1967). The average excess duration was ~10 min; the threshold energy of the particle detector was ~100 keV. The Italian EAS-TOP surface array (Aglietta et al., 1989) measures significant excesses in the air shower count rate lasting 10–20 min. The enhancements with maximum amplitude of 10%–15% were attributed mostly to the highest energy Extensive Air Showers (EAS; large shower sizes, $>10^6$ electrons), and to zenith angles of incidence smaller than 20°; "thickness" (time interval of the EAS particles arrival) of shower was slightly larger than in normal conditions (Vernetto et al., 2001).

A radiation monitoring post in a nuclear power plant in Japan reports on a comprehensive observation of a gamma ray burst emission lasting less than 1 min—correlated with snow and lightning activity. Enhancements were detected only during wintertime, when thunderclouds are as low as several hundred meters (Torii et al., 2002). The same group observed a summer thunderstorm at the top of Mount Fuji (3776 m high). The flux of high-energy gamma rays had continuous energy spectrum up to 10 MeV, prolonged up to 20 min. The authors of Torii et al. (2009) claim that the bremsstrahlung photons generated by the energetic electrons were produced continuously due to an intense electric field in the thundercloud rather than having originated in the process of lightning discharge.

A Japanese group on another Japanese power plant also detected short (less than 1 min) gamma ray bursts during winter thunderstorms (Tsuchiya et al., 2007). The same authors reported a simultaneous detection of gamma rays and electrons at a mountain observatory Norikura located 2770 m above sea level (Tsuchiya et al., 2009). Two emissions, lasting 90 s, were associated with thunderclouds. At the same research station at Norikura in the Japanese Alps a large multilayered particle

* Corresponding author.
E-mail address: mbagrat@gmail.com (B. Mailyan).

0169-8095/$ – see front matter © 2012 Elsevier B.V. All rights reserved.
doi:10.1016/j.atmosres.2012.05.008

detector operates, primarily intended to register solar neutron events. In August 2000 on account of thunderstorms, particle flux enhancement was detected in 3 layers of a 64 m^2 area detecting system (Muraki et al., 2004).

In experiments at the Baksan Neutrino Observatory of the Institute for Nuclear Research, the time series of hard and soft components of secondary cosmic rays are continuously measured along with measurements of the electric field and monitoring of thunderstorms. Intensity changes of the soft cosmic rays (below 30 MeV) and hard component (>100 MeV) were studied (Lidvansky and Khaerdinov, 2009). It was shown that the critical field and particle energy for this process are ~300 kV/m and ~10 MeV respectively (Khaerdinov et al., 2005).

A network of the NaI detectors along with EAS triggering system is located at Tien-Shan Cosmic Ray station of the Lebedev Physics Institute, at altitude of 3340 m. The goal of the research is to detect runaway breakdown initiated by EAS with energy above 1000 TeV—so-called RB-EAS discharge. Based on short gamma flashes (less that 200 μs) detected by the network of gamma ray detectors, the authors of Gurevich et al. (2009) claim that RB-EAS discharge is a rather rare event — occurring in only ~1% of all EAS registered during thunderstorms, requiring coincidence of several conditions. The most important of them being that the strong electric field should be located not higher than 400–500 m above the detector.

Recently Japanese groups perform new measurements of gamma ray emission and detect the source of the radiation in thundercloud moving across locations of several nuclear power plants (Torii et al., 2011; Tsuchiya et al., 2011).

Facilities of the Aragats Space Environment Center (ASEC) (Chilingarian et al., 2003, 2005) observe charged and neutral fluxes of secondary cosmic rays by the variety of particle detectors located in Yerevan and on slopes of Mount Aragats at altitudes 1000, 2000 and 3200 m. ASEC detectors measure particle fluxes with different energy thresholds as well as EAS initiated by primary proton or stripped nuclei with energies greater than 50–100 TeV (Chilingarian et al., 2010). Abrupt enhancements of particle detector count rates correlated with thunderstorm activity, so called Thunderstorm Ground Enhancements (TGEs) detected during 2008–2011 bring vast amounts (243 TGE events) of small and very few large TGEs (only 6 TGE events with amplitude exceeding 20%) allowing the detailed analyses and taxonomy of the new high-energy phenomena in the atmosphere.[1] The flux enhancement is presented in percent relative to rather stable background of the ambient population of secondary cosmic rays. As we can see in the left corner of the histogram (Fig. 1), majority of TGE events have amplitude less than 10%. These small TGEs and analogical TGEs reported by other groups can be explained by the modification of the energy spectra of charged particles in the electric field of thunderclouds. Due to asymmetry of positive-to-negative flux of secondary cosmic rays in the terrestrial atmosphere, peaks and dips can arise in time series of count rates of surface particle detectors. These effects have been theoretically analyzed in Dorman and Dorman (2005) and detected on Mount Norikura (Muraki et al., 2004) and in Baksan, Russia (Alexeenko et al., 2002). Measurements at ASEC and simulations with GEANT4 package (Agnsotelli et al., 2003) confirm additional flux of gamma rays up to 1000% in the energy range of 2–20 MeV and up to 10% in the energy range up to 100 MeV. Simultaneously dips in the muon flux at energies above 200 MeV were obtained by GEANT4 simulations and detected by ASEC detectors.

Few very large enhancements seen in the right corner of Fig. 1 can be explained only by invoking the Runaway Breakdown (RB) process (Gurevich et al., 1992), also referred as Relativistic Runaway Electron avalanche (RREA, Dwyer, 2003, 2007; Carlson et al., 2008). Ambient population of secondary cosmic ray electrons in the electric fields with strength greater than the critical value[2] unleashes the electron-gamma ray avalanches and total number of particles on the exit from cloud can be multiplied by several orders of magnitude. Proceeding from the measurements of the charged and neutral fluxes as well as from the energy deposit of particles in thick scintillators, we recover the energy spectra of TGE electrons and gamma rays for the 2 largest TGE events of September 19, 2009 and October 4, 2010. Installation of Aragats field meters (Boltek firm electric mill EFM100, http://www.boltek.com/efm100.html) and lightning detectors (LD250 powered by the software from Astrogenic systems, http://www.boltek.com/ld250.html) allows correlating the measured particle fluxes with near-surface electric field disturbances and with occurrences of lightning of different types.

In Fig. 1, we present the histogram of the 243 TGE amplitudes (relative enhancements above cosmic ray background) measured by the MAKET detector in 2008–2011; the dates of 4 largest TGE events are displayed as boxed text. Lightning occurrences, as well as sketch of the RREA process in upper and lower dipoles also are depicted. The indispensible condition of TGE initiation is the creation of the lower dipole accelerating electrons downward. The temporarily emerging lower positive charge region (LPCR, Qie et al., 2009) is smaller than the mid-level negative and upper positive layers of the main upper thundercloud dipole (Williams, 1989). Therefore TGE phenomena are local and its duration coincides with the duration of the LCPR, which is usually ~10 min.

The critical electric field strength for the conventional discharge in thunderclouds is very large (~10 times more than RREA critical field) and was never measured in thunderclouds. Therefore, electron-gamma ray avalanches could initiate lightning by creating the initial conductive channel (Gurevich et al., 1999; Dwyer, 2005). Lightning in turn can provide the RREA process with additional seed electrons from the current pulses along developing lightning leader channels (Carlson et al., 2009; Lu et al., 2010, 2011; Cummer et al., 2011).

For the Terrestrial Gamma-ray Flashes (TGFs, Fishman et al., 1994) the physical model is symmetric. The electrons are accelerated upward by the negative field between main negative layer in the middle of the cloud and main positive layer near the top of the cloud. The additional seed electrons are provided by the positive intracloud lightning occurrences usually accompanying the detection of TGFs by the orbiting

[1] Time series of changing particle fluxes registered from ASEC monitors, as well as magnetometer and electrical mill measurements are available from http://adei.crd.yerphi.am/adei/.

[2] The critical electric field E_t = 1.534; 1.625, and 1.742 kV/cm at 4500, 4000 and 3400 m respectively. E_t dependence on altitude follows the air density dependence on altitude.

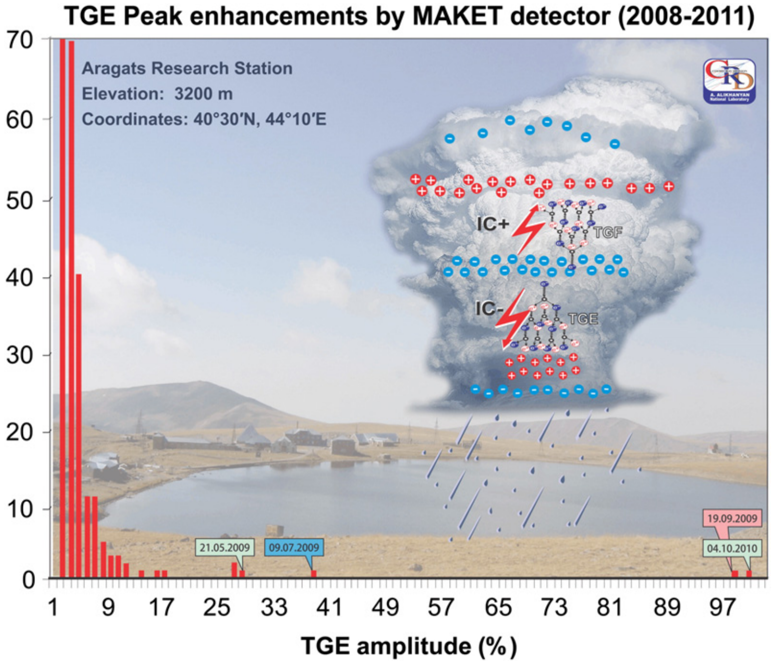

Fig. 1. The histogram of the amplitudes of TGE events detected by ASEC detectors in 2008–2010. The peak values of the cosmic ray flux increase above rather stable secondary cosmic ray background were measured by the outdoor plastic scintillators.

gamma ray observatories (Stanley et al., 2006; Cummer et al., 2005).

2. Dynamics of TGE events

Despite big varieties of measurements in the thundercloud electric field profiles the following basic structure of the electric field in thunderclouds is widely accepted: from the ground up to the cloud base there is usually a low magnitude field (both positive or negative); relatively small positively charged "pocket" (comprising only ~20% of negative charge higher) is responsible for the larger positive field prolonged up to negatively charged layer at 1–2 km above cloud base; and the negative field is extended about 1–4 km above the negative layer where the main positive charge is located (Stolzenburg et al., 1998). In presence of the positive electric field (pointed upward)[3] within the cloud, the electrons are accelerated downward and, dependent on the strength of the field, the flux of electrons and gamma rays reaching earth surface may exhibit significant amplification. As shown in Fig. 1, most of TGE events have rather small amplitudes; sometimes (less often than once per year) under yet fully unknown conditions the RREA process is unleashed and surface detectors measure huge TGEs surpassing rather stable cosmic ray background flux several times. The necessary condition for the RREA process is the creation of the considerably large positively charged layer in the bottom of the cloud. The manifestation of the existence of such layer is the absence of the cloud-to-ground lightning occurrences (leader attempts) due to the "blocking" of descending negative leader from reaching the ground. Simultaneously, significant enhancement of the intracloud negative lightning (Cui et al., 2009) occurrences took place due to the "converting" potential of the cloud-to-ground flash to an intracloud one (Nag and Rakov, 2009). On May 27, 2011, we detected a large TGE event by the 5 NaI crystals of size $30\times12.5\times12.5\ \mathrm{cm}^3$ newly installed at Aragats.

In Fig. 2, we can see the abrupt increase of the near-surface electric field at 13:07 UT caused by the negative cloud to ground (−CG) lightning flash that contained several strokes to the ground; thereafter the polarity of the electric field starts to reverse.[4] After 13:08 UT the TGE started (green curve) and −CG lightning occurrences stopped after 13:10 UT. At 13:12–13:15 UT we detect numerous intracloud negative discharges (−IC) in radii of 3 km, suggesting the screening of the ground by lower positive charge region (LPCR). The lightning stepped leader may provide the RREA process with additional seed electrons (by the "cold" runaway process, Moss et al., 2006) and at 13:12–13:15 UT the gamma ray intensity peaked at ~70% level above the background when the near surface electric field reaches its minimum.

The LPCR with main negative layer in the middle of the cloud forms lower dipole, responsible for the downward electron acceleration and also playing major role in initiation of cloud-to-ground (−CG) and intracloud (−IC) lightning

[3] We adopt the "atmospheric electricity" sign convention: the positive field (E kV/m) accelerates electrons downward in the direction of the Earth; the negative field (−E kV/m) vice-versa accelerates electrons upward in the direction of space.

[4] The rapid changes of the near-surface electric field usually are accompanied also with rapid change of the electric field within thundercloud (Standler and Winn, 1979).

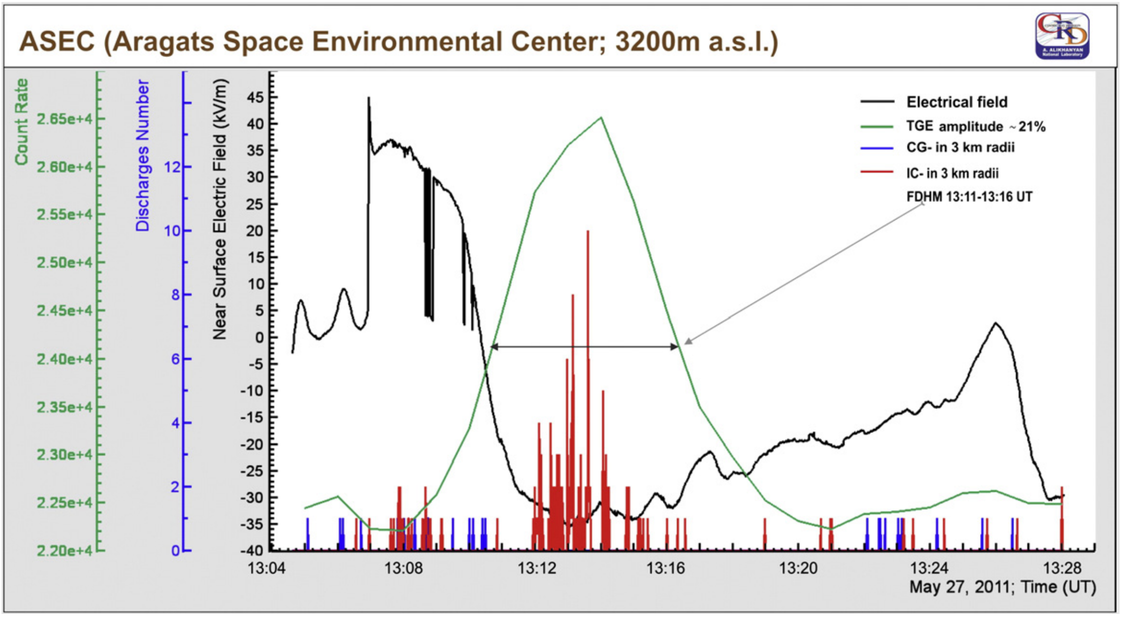

Fig. 2. The near-surface electric field (black curve) and frequency of lightning occurrences measured by the Bolter detector each second (2 left vertical axes). 143-CG— lightning occurrences were detected at 13:05–13:10 UT in the radii of 10 km (blue) and 139 IC— lightning occurrences — at 13:12–13:15 UT, radii of 3 km (red). Time series of the NaI crystals count rate (green curve, right vertical axes) demonstrate ~70% enhancement on May 27, 2011 at Aragats, 3200 m a.s.l. (For interpretation of the references to color in this figure legend, the reader is referred to the web version of this article.)

occurrences. Many researchers outline the dominant role that LCPR plays in initiating/triggering an intracloud and cloud-to-ground lightning discharges (Pawar and Kamra, 2004; Nag and Rakov, 2009; Qie et al., 2009). We suggest that development of the LCPR also has a major role in TGE initiation. The locality of the RREA can be explained by the small sizes of the lower positive charge region and the transient character of LCPR can explain the duration of the TGE. Based on the detection of the winter thunderstorms by Japanese authors of Tsuchiya et al. (2011), they estimate the radii of the circle of intense RREA radiation to be 600 m. Another Japanese group (Torii et al., 2011) detects moving at the speed of 7 m/s energetic radiation source at the height of 300 m along with the negatively charged region within the thundercloud at the height of around 1 km. The radiation was emitted from a downward hemispherical surface with radii of 700 m. These findings demonstrate the locality of the RREA process and imply that the number of additional gamma rays can vary significantly depending on the “impact parameter” of the thundercloud relative to the detection site (see also Babich et al., 2010).

Therefore, it is not always the lower dipole that initiates TGE; an evidence of the emerging LPCR without initiated TGE can be seen in Fig. 3. On June 8, 2011, the fair weather field was changed by moderate positive field at 11:29 UT; then electric field reversal happened at ~11:33 UT and field reach negative value was ~−30 kV/m. At 11:55 UT, electric field abruptly changes the polarity and simultaneously the (−CG) lightning occurrences stopped and the intracloud negative lightning (−IC) occurrence started. From Figs. 2 and 3, using the model sketched in Fig. 1, we can conclude that the creation of LCPR stopped −CG lightning occurrences and initiated −IC lightning occurrences. At the same time, near surface electric field changes the polarity and turns from positive to negative. It is also worth mentioning that during this thunderstorm we do not observe any significant TGE in charged and neutral fluxes. The reason of it can be the much higher intensity of the −IC lightning occurrences, comparing with May 27 TGE, which does not allow the development of the mature RREA process. Another reason can be the distant location of the positive bottom layer; only if the positive layer is above the detectors the RREA process can accelerate electrons downward in the direction of the observer.

Continuous measurements of the lightning activity, near-surface electrical field and particle fluxes give a possibility for the first time to investigate the interrelations of these geophysical parameters and estimate the intracloud (IC-) to cloud-to- ground (CG)-lightning flash ratio (Z, Pinto et al., 2007; De Souza et al., 2009) during thunderstorms at Aragats. The Z ratio gives information about the electrical activity in thunderstorms and can be a clue about how the centers of the charge are disposed in the clouds. Our finding that Z is peaked at the minimal near-surface electrical field and the maximum of RREA particle flux confirms that Z is directly correlated with LPCR development.

In Fig. 4, we demonstrate another type of the TGE event: relatively small near-surface electric field and absence of any kind of lightning occurrences accompanied by the moderate count rate enhancement. At 8:35 UT, October 16, 2010 we observe abrupt decrease of the electric field, followed after 2 min by a ~7% enhancement of the count rate of the outdoor plastic scintillators. No lightning occurrence within 10 km was observed during ~10 min of negative field duration and TGE detection.

As the strength of the near-ground electric field was 2 times less than at 27 May and there were no lightning occurrences we can assume that the LCPR was not well developed, and RREA process was not started.[5] The TGE initiation at 16 October can be connected with Modification Of the energy Spectra

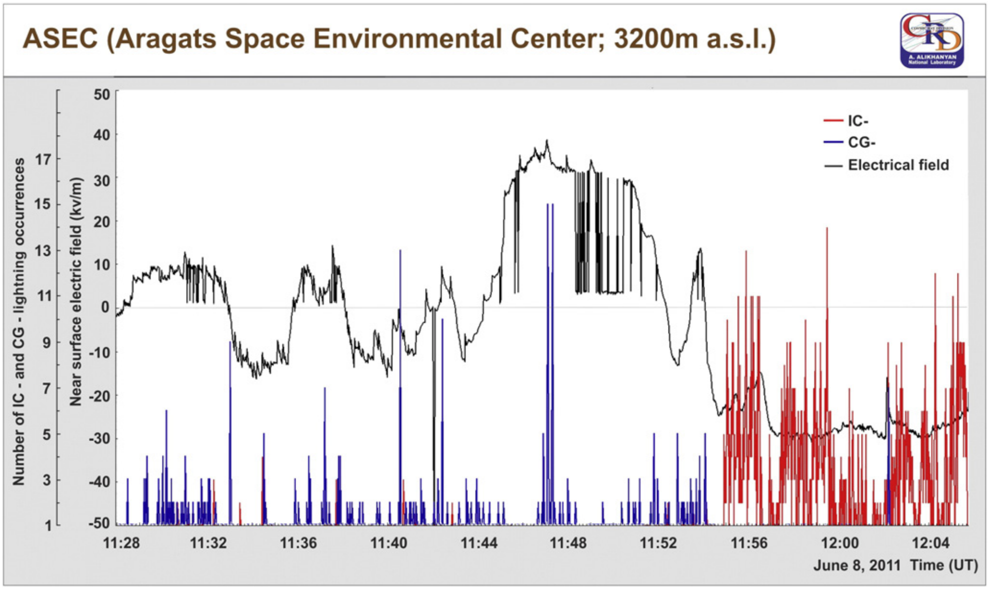

Fig. 3. The disturbances of near-ground electric field and frequency of cloud to ground (−CG) lightning occurrence at Aragats, 3200 m on June 8, 2011.

(MOS) of charged cosmic rays entering the region of the strong electric field within the thundercloud. Thus we introduce 2 types of the TGE origin: RRE avalanches responsible for very rare huge particle multiplication in the thunderclouds (up to 1000%) and MOS process — responsible for much often but small and modest (less than 10%) TGEs.

3. Acceleration and deceleration of the secondary charged cosmic rays in weak electric fields

From the consideration of the three thunderstorm events above, we can conclude that by no means electric fields in thunderclouds ultimately result in TGE, and far not all TGEs are due to RREA process. In the database of ASEC time series, we can find significant non-random variations of cosmic ray intensity in the absence of any lightning occurrences, indicating that the electric field strength in the cloud is below the RREA threshold. In Dorman and Dorman (2005), the theory of the modulation of the secondary cosmic ray by the various meteorological effects, including strong electric fields within thunderclouds is developed. Electrons and negative muons are accelerated downwards by a lower dipole before reaching particle detector. The positrons and positive muons as well as protons will be decelerated in the lower dipole. The positive charge of primary cosmic rays (mostly protons and stripped nuclei) introduces several asymmetries between particles and antiparticles born in atmospheric cascades. The intensity of the MeV electrons is larger than the intensity of positrons of the same energies in energy range of 1–50 MeV; the intensity of positive muons above 100 MeV is larger than the intensity of the negative muons, see Figs. 5 and 6 (obtained by EXPACS package, Sato et al., 2009).

We can see in Fig. 5 that the number of electrons with energies below 50 MeV at 5000 m altitude is significantly larger than the positrons. It means that positive electric field in the thundercloud will significantly alter the total intensity of low energy charged particles registered by scintillators at the Earth surface. The changes of intensity will manifest themselves as peaks and dips in the time series of count rates of particles registered by the scintillators located on the Earth surface. The energy spectrum of electrons will be shifted to the right (mean energy becoming larger) leading to the additional bremsstrahlung gamma rays; energy spectrum of positions shifted to the left is not sufficient to compensate these enhanced counts. The attenuation of the electrons in the atmosphere is much larger than the one of the gamma rays. Therefore, most TGE events are detected in the fluxes of gamma rays born by accelerated electrons.

Interestingly, positive fields have opposite influence on counts of muons at energies above 200 MeV. Among ASEC particle detectors there are scintillators with energy threshold greater than 200 MeV and the electron acceleration described above will not influence their count rate. Due to the abundance of the positive muons over the negative muons (1.2–1.3 times, at 100–500 MeV energies, Wentz et al., 2003, see Fig. 6) the braking of positive muons in the positive electric field cannot be compensated by the acceleration of the negative muons in the same field. The consequences of this asymmetry are indicated in Fig. 7. On October 4, 2010, we detected ~5% deficit in the flux of muons with energies greater than ~200 MeV, which concurred with a huge excess of low energy gamma rays and electrons.

[5] Of course, the combination of measurements on the microsecond scale of the lightning occurrences of different types and of the TGE in electron and gamma ray fluxes, as well as the electric field strength within the thundercloud is needed for the definite conclusion on the interrelations of these phenomena.

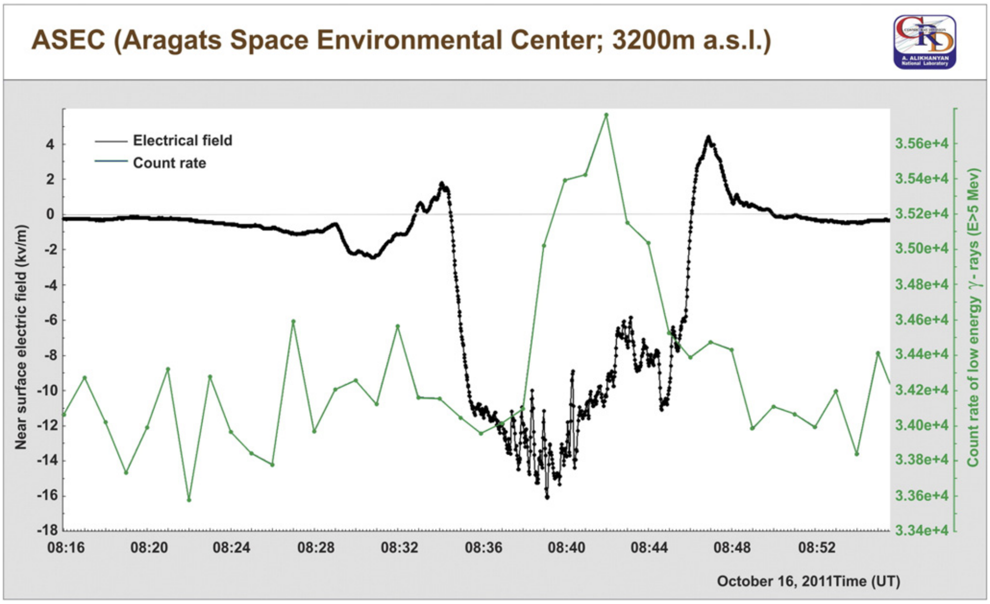

Fig. 4. The TGE event on 16 October 2010, the bold black line is the near-surface electric field strength; the gray line is the minute count rate of the 3 cm thick outdoor scintillator (energy threshold 4 MeV).

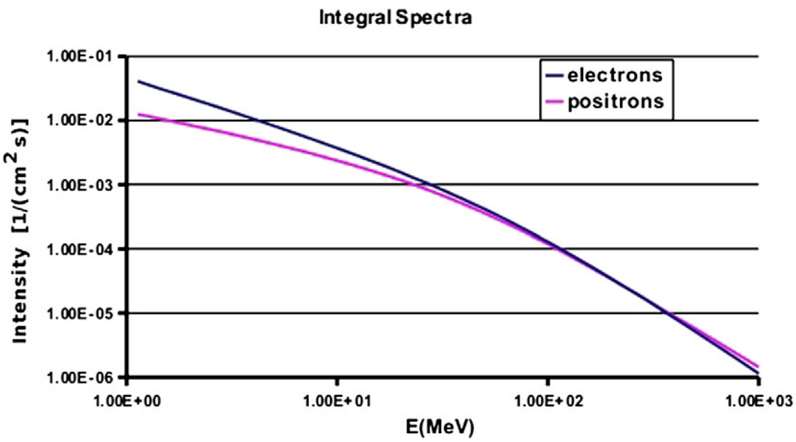

Fig. 5. The energy spectra of electrons and positrons at altitude of 5000 m a.s.l.

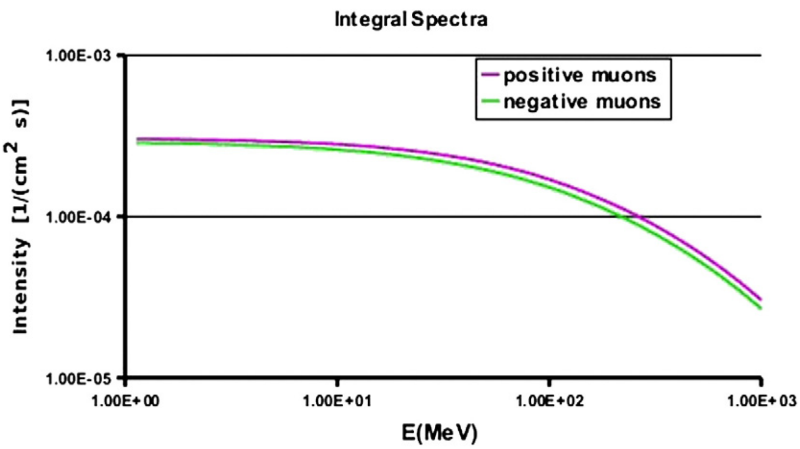

Fig. 6. Energy spectra of muonsat altitude 5000 m a.s.l.

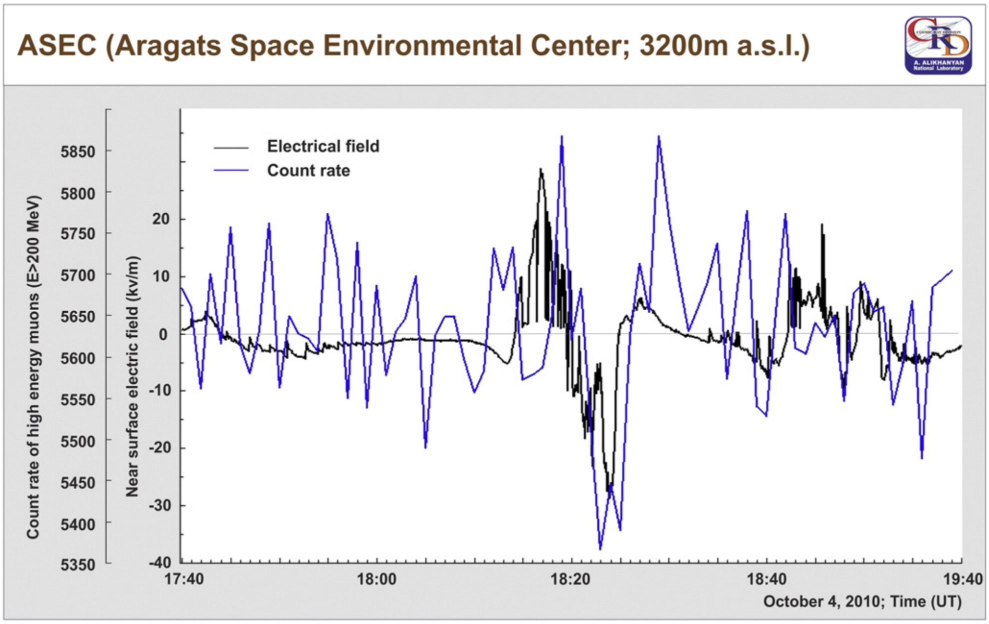

Fig. 7. The positive field in the thundercloud (electrons are accelerated downwards) stops positive muons; charge ratio of positive-to-negative muons is ~1.2–1.3, therefore we detect ~5% deficit of the flux of high-energy muons (energy > 200 MeV); simultaneously huge TGE in gamma ray and electron fluxes were measured.

4. GEANT4 simulations of particle propagation in strong electrical fields of thunderclouds

To get clues in the mechanisms of electron acceleration in the thunderclouds we implement simulations using a simple model of the electric fields in the thundercloud. GEANT4 simulations of the particle propagation in thunderclouds were performed with an electric field of 1.8 kV/cm spread uniformly from 5000 m till 3600 m a.s.l. Secondary Cosmic Ray (CR) electrons as seed particles in the energy range of 1–300 MeV and with fixed energy 1 MeV (simulating "pure" RREA process, ~1 MeV electrons commit minimal ionization losses in the atmosphere) were used. We chose the uniform electrical field strength above the critical energy of the RREA process at altitudes from 5000 m to 3400 m (1.7 kV/m) and fields below this threshold to illustrate the influence of the modification of secondary CR particle spectra (MOS process), as was described in the previous section.

In Fig. 8, we can apparently see 2 modes of particle generation. The RREA mode with maximal energy of electrons is 30–40 MeV and gamma rays — 20–30 MeV and MOS mode accelerating electrons up to 60–70 MeV; gamma ray spectrum prolonged up to 80–90 MeV. The electron and gamma ray energy spectra in the energy range of 1–10 MeV demonstrate large multiplication of electrons in the RREA process and huge amplitudes of the TGEs. MOS regime is fast fading after 50 MeV and needs large surfaces of particle detectors to be measured above the background of ambient population of secondary cosmic rays.

The high-energy tail of the gamma ray spectrum is due to enhanced bremstrahlung radiation of the higher energy electrons traversing the electric field of the cloud. Because of the highly enlarged radiation losses, high energy electrons cannot unleash the RREA, however, the additional flux of gamma rays radiated by these electrons can reach the mountain altitudes and be registered as small and modest enhancement over CR background — see the histogram in Fig. 1.

To prove our hypothesis on 2 component origin of TGE, we perform the same simulation with a fixed flux of 1 MeV seed electrons. The shape of electron and gamma ray spectra coincides with spectra obtained with 1–300 MeV electron seeds (exponential function — reflecting the particle multiplication in the avalanche process), however there are no high energy tails, see Fig. 9. Thus, pure RREA process with chosen electrical field parameters cannot produce TGE electrons with energies above 30–40 MeV and gamma rays with energies above 20–30 MeV.

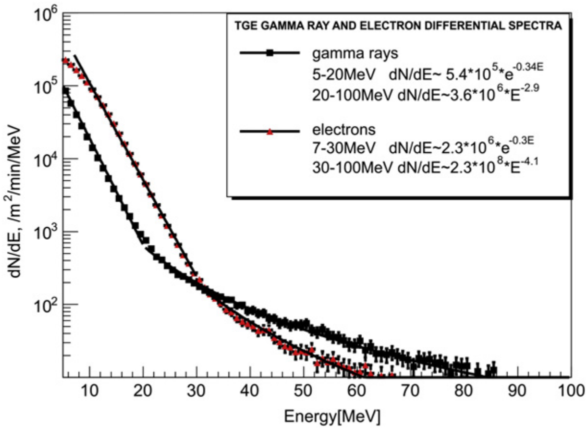

Fig. 8. TGE electron and gamma ray spectra obtained from GEANT4 simulation of RREA process in an electric field of 1.8 kV/cm with seed electrons of 1–300 MeV.

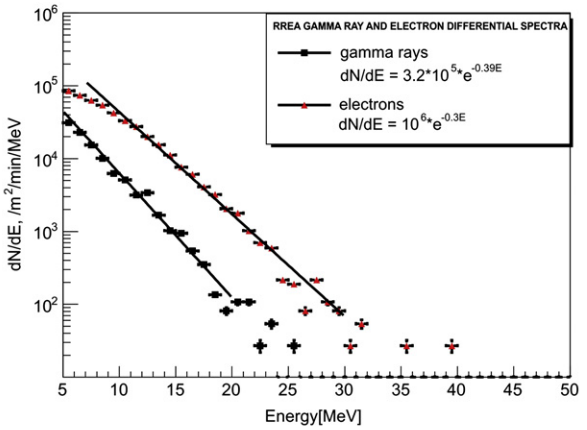

Fig. 9. The electron and gamma energy spectra obtained in electric field of 1.8 kV/m prolonged from 5000 till 3400 m with 1 MeV electron as seeds.

To prove that MOS process can provide high-energy gamma rays we perform simulations of the electron propagation in the moderate electric field below RREA initiation threshold (1.5 kV/m). In Fig. 10 we see that only the modification of the energy spectra of electrons can significantly enlarge the yield of the gamma rays reaching the earth surface. Electrons attenuate in the atmosphere after exiting from the cloud; however, as we can see from Fig. 10, the gamma rays survive.

5. The energy spectra of TGEs

5.1. TGE electron spectrum

The ultimate check of the RREA process detected on the ground is the measuring of the energy spectra of electrons and gamma rays well above the background of cosmic rays. Among hundreds of TGE events detected at ASEC only September 19, 2009 and October 4, 2010 TGEs allow the electron energy spectra recovering. After the estimation of the gamma ray flux, we subtract the obtained gamma-ray contamination, taking into account the efficiencies to register gamma rays by the particular detector and recover electron integral energy spectrum using several detectors with different energy thresholds. In Fig. 9, electron spectra of September 19, 2009 and October 4, 2010 TGEs are presented. The spectrum of September 19, 2009 TGE was obtained by additional counts of plastic scintillators with energy threshold of 9, 12, 15, 18 and 25 MeV (52, 826, 21,773, 15,967, 6750 and 506 electrons per minute per m^2, were registered respectively). The spectrum was approximated with exponential function (see fit parameters in the legend of Fig. 9); corresponding exponential mean energy equals to ~3.3 MeV. Scintillators with thresholds of 2, 7 and 12 MeV (36,089, 3896 and 459electrons per minute per m^2,was registered correspondingly) were used to recover the October 4, 2010 TGE electron integral spectrum; for this event the mean energy equals to ~2.3 MeV; both values are significantly smaller comparing with estimates based on simulations of the RREA (Lehtinen et al., 1999; Dwyer, 2004, ~7.2 MeV); however the 7.2 MeV value was obtained for the electrons just exiting the electrical field and for rather large electrical field strengths, 2 considered measurements at Aragats were made according to our estimates 50–150 m below the thundercloud (Fig. 11). For the details of separation of electrons and gamma rays and October 4, 2010 TGE electron spectrum recovery, see Appendix A.

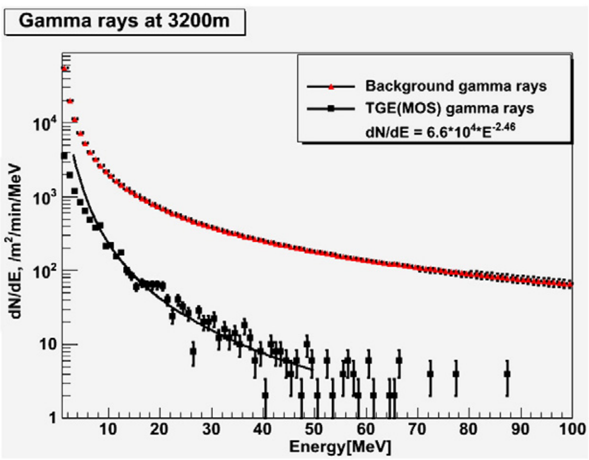

Fig. 10. Comparison of background gamma ray spectrum with the surplus gamma ray spectrum generated by electrons accelerated in the field of strength 1.5 kV/m below the critical field for the RREA initiation; the background cosmic ray gamma ray flux and TGE gamma ray flux are calculated at 3200 m altitude after exiting from the uniform electrical field at 3350 m altitude.

5.2. The energy spectra of the TGE gamma rays

The energy spectra of September 19, 2009 and October 4, 2010 TGE gamma rays are recovered based on the energy deposit spectra measured by Cube and ASNT detectors (see details of detector operation in Chilingarian et al. (2010) and details of spectra recovery in the Appendix B). Both Cube and ASNT detectors are measuring the energy deposit histograms and store them each minute. These histograms reproduce the

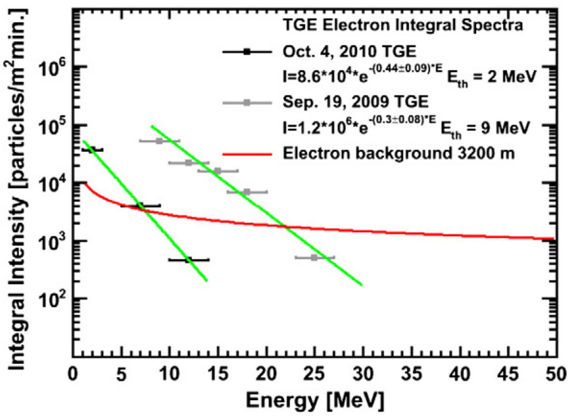

Fig. 11. Electron integral energy spectra of the September 19, 2009 and October 4, 2010 TGEs measured at 3200 m compared with the energy spectrum of the ambient population of the cosmic ray electrons at the same altitude (background).

energy spectrum of gamma rays, however they are folded by the detector response very differently for Cube and ASNT detector assemblies. Recovering the energy spectrum by the energy deposit histograms, i.e. solving the inverse problem of cosmic ray physics is rather a complicated task and we use multiple trial spectra for solving it (see for details Appendix B). The outdoor Cube detector was installed at Aragats in Spring 2010, near MAKET building, providing lower threshold of detected particles than indoor detector ASNT. Thus, only for October 4, 2010 TGE, we recover the gamma ray energy spectrum in the range of 5–10 MeV. The spectrum was approximated by both exponential and power law functions. Exponential function with mean energy of ~3.8 MeV provides slightly better approximation of the measured energy deposit with simulated one, than power law fit with index −1.8. χ^2/ndf were ~2 and ~3 for the exponential and power functions respectively.

Since the maximal energy deposit in Cube detector is less than 40 MeV (the scintillator thickness is only 20 cm, comprising ~0.5 radiation lengths), we can reliably recover the spectrum at energies higher than 40 MeV with the ASNT detector assembly only (4 independent detectors comprising scintillators of 60 cm thickness, ~1.5 radiation length).

We use the Cube energy deposit spectra for the calibration of ASNT detector response. By the energy deposit spectra measured by Cube detector we cannot estimate the maximal energy of the gamma rays. We use the energy deposit spectra measured by ASNT to decide on the maximal energy of the gamma ray spectra (see Appendix B). Above 10 MeV the energy spectra are better approximated with power law. The spectral indices of gamma ray differential energy spectra were estimated to be 3.3 ± 0.7 and 3.4 ± 0.25.

The recovered gamma ray energy spectra posted in Fig. 12 have no error bars due to the spectra recovering method; we chose a particular power index (the power was found to be the best model), which provides simulated energy deposit histogram (obtained by simulation of the detector response) closest to the experimentally measured one (see details in Attachment B). The uncertainties of the procedure, including the possible errors in estimating detector response are included in the errors of the estimated power law indices.

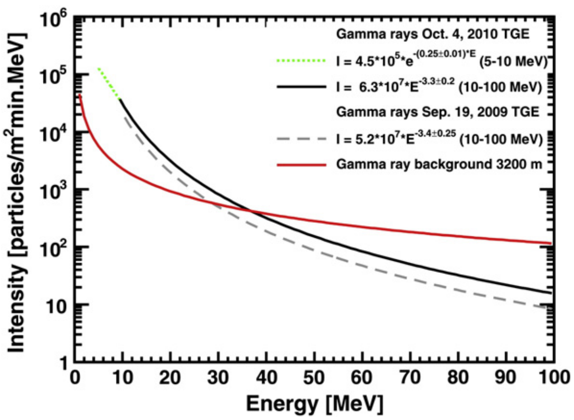

Fig. 12. The differential energy spectra of the gamma rays detected on September 19, 2009 and October 4, 2010.

6. Discussion and conclusion

The high elevation (~3200 m) of ASEC provides a good opportunity to detect thunderstorm-correlated particles, which attenuate rapidly in the atmosphere. We measure fluxes of the RREA electrons and gamma rays with intensities ~10 times above the cosmic ray background, thus, proving the existence of the runaway mechanism in thunderstorm atmospheres theoretically predicted by Gurevich et al. (1992). Both electron spectra measured on September 19, 2009 and October 4, 2010 are exponential. The gamma ray spectrum in the energy range 5–10 MeV (4 October 2010 TGE) also is better fitted with exponential function, in agreement with our simulations, see Fig. 9.

The estimated mean energies of the electron integral spectra are equal to ~2.3 and 3.3 MeV for October 4, 2010 and September 19, 2009 TGEs. The mean energy of the gamma ray differential energy spectrum in the energy range of 5–10 MeV is estimated to be 3.8 MeV.

It is less than derived from the simulations that the values of mean equal to 7.2 MeV (Dwyer, 2004). However, these values are in good agreement with values obtained from our simulations. Values of the mean energy of the 3 brightest electron/positron Terrestrial gamma flashes (TGFs) measured by the GBM, Fermi also are less than 7.2 varying from 2.3 to 4.6 MeV (Briggs et al., 2011).

Power law describes gamma-ray spectra at energies higher than 10 MeV. The energy spectra of the gamma rays extend till 100 MeV and demonstrate no exponential cutoff at high energies as obtained in many simulations of the RREA process (Dwyer and Smith, 2005). We suggest that the modification of the cosmic ray electron energy spectra in the electric field of the thundercloud leads to additional bremsstrahlung radiation reaching the Earth and sustaining the tail of TGE gamma ray spectra (the MOS process). As the cosmic ray spectra are power law, the high-energy tail of TGE gamma ray spectra is also a power law.

In the discussion section of Chilingarian et al. (2010), we estimate the height of thundercloud on September 19, 2009 TGE by assuming the maximal energy of RREA electrons ~50 MeV and calculating the distance in the air in which these electrons will lose 20–25 MeV (the maximal energy of measured electrons of September 19, 2009 TGE was estimated to be 25–30 MeV). After simulating the RREA process we come to the estimate of maximal energy of RREA electrons to be 30–40 MeV. Therefore we have to re-estimate the thundercloud elevation above detectors on September 19, 2009. Also we introduce a parameter, namely the ratio of electron to gamma ray flux, for estimation of the cloud (electric field) height, see Appendix C. With newly estimated thundercloud height, we re-estimate several phenomenological parameters of the RREA process as the following: the most probable height of thundercloud (and electrical field therein) is ~50 m. The number of electrons with energies above 1 MeV at the exit from the cloud is $1.97 * 10^7$ electrons/m^2/min; if we assume that the radiation region in the thundercloud has a radius of 1 km the total number of electrons crossing this region in a minute is $\sim 6 * 10^{13}$.

The same method applied to October 4, 2010 TGE gives the thundercloud height of 130 m. Taking into account that maximal energy of the detected electrons on October 4 was

12–14 MeV, we come to the estimate of the maximal energy of the RREA electrons to be 30–40 MeV, which is in good agreement with our simulations (Fig. 9). The most probable height of thundercloud (and electrical field therein) is ~130 m. The number of electrons with energies above 1 MeV on the exit from the cloud is ~$1.5*10^9$ electrons/m^2/min; if we assume that the radiation region in the thundercloud has a radius of 1 km the total number of electrons crossing this region in a minute is ~$5*10^{15}$.

The dynamics of the TGE increase (shown in Fig. 2) suggests that the largest TGE started by RREA having as seed particles the secondary cosmic ray MeV electrons; the particle avalanche developing in the direction to the Earth from the main negative charge layer in the middle of the thundercloud may create the initial conductive channel for the negative intracloud lightning discharge (Babich et al., 2011). The −IC lightning in turn may provide RB process with additional seed electrons from the current pulses along developing lightning leader channels thus enhancing the intensity of the electron and gamma ray fluxes.[6] Detection of the −IC lightning occurrences during the TGE events supports the suggested model. However, we recognize that the time scales of the lightning and TGE are drastically different and for definite conclusions on the possible seeds from the stepping leader we should compare on microsecond time scale the particle fluxes and lightning occurrences. Nonetheless the discovery of very short (less than 50 μsec) particle bursts within TGEs, coinciding with minute of the maximal flux (see for details, Chilingarian et al., 2011), illustrates the possible link between TGE and lightning.

The scenario of the TGF initiation is symmetric to the TGE: the electron-gamma avalanche is developing upward from the main negative charge layer to the main positive charge layer; coming out of the cloud, gamma rays are moving by straight lines to be detected by the orbiting gamma ray observatories. TGF gamma rays on their way to orbiting gamma observatories generate by Compton scattering and pair production high-energy electron-positron beams (TEBs, Dwyer, 2012), which follow the geomagnetic field line in the inner magnetosphere and may be observed thousands of kilometers away. The RREA developed in the upper dipole usually initiates positive intracloud lightning IC+ (Cummer et al., 2005; Shao et al., 2010; Lu et al., 2010) and the stepping leader of lightning may provide the RREA process with vast numbers of seed electrons.

7. Possible systematic errors

We do not measure the electric field within the thundercloud; near surface electric field is not a good proxy of the intracloud fields accelerating electrons downward. We also do not measure vertical extension of the field and only estimate the height of the cloud. Therefore, simulations of the RREA process in the atmosphere with chosen parameters, although are in an agreement with the available measurements of electric fields in the thunderclouds, cannot be used for direct comparisons with TGE measurements. However, these simulations give us understanding of the RREA scale and MOS processes and expected behavior of the energy spectra.

The radiation length of the ASEC electromagnetic calorimeters is 0.5 for Cube and 1.5 for ASNT, light attenuation in the thick scintillator significantly decreases the light incident on the PM cathode, and consequently the PM output pulse. Nonetheless, due to large gamma ray fluxes, energy deposit histograms collected during 1 min of peak intensity give a possibility to recover differential energy spectra of the gamma rays. To check the obtained gamma ray spectra and used attenuation coefficients several calorimeters were used for inter-calibration.

Due to particle bursts (Chilingarian et al., 2011) incident on colorimeter several large energy deposits may be because of multiple particle traversals. These effects are difficult to simulate and our method of the multiple spectra testing can give optimistically biased maximal energy of TGE gamma rays. Therefore, we do not include in the energy spectra recovering procedure 2 largest bins of the energy deposit histogram.

The electron/gamma separation is made by using veto scintillators with non-zero efficiency to detect charged flux. Nonetheless multilayered detectors with dedicated coincidence logic help to check the estimated fraction of TGE electrons and gamma rays and make appropriate corrections.

Several detecting devices are placed at high altitude, under snow and strong winds and it is very difficult to keep stable detecting channel parameters (high voltage, electronics thresholds and other) influencing the operation of detectors. However, high altitude station staff maintained detector operation 24 h daily for 12 months yearly and on-line visualization programs ADAS (Chilingaryan et al., 2008) and ADEI (Chilingaryan et al., 2010) provide possibilities of the remote monitoring and control of the key parameters of detectors.

8. Conclusions

We introduce 2 component model of the TGE origin: the RRE avalanches in energy domain up to 30–40 MeV and Modification Of energy Spectra (MOS) process operating on all energy scales and providing extension of gamma ray energy spectra up to 100 MeV. The RREA process can multiply particle flux up to 10 times above ambient background of secondary cosmic rays; the MOS process can provide several percent excess above cosmic rays, however for the much higher energies.

The TGE process is well correlated with near-surface electrical field and with lightning occurrences. All TGEs occur at the large negative near-surface electrical field and particle flux is accompanied with intracloud lightning occurrences (IC−) and suppression of cloud-to-ground lightning occurrences (CG−)). Measured structure of lightning occurrences supports creation of developed lower positive charge region (LPCR) as a fundamental condition of TGE origination.

Acknowledgements

This work was partly supported by the Armenian government grants, NFSAT-CRDF-ECSP-09-69 grant and by ISTC A1554 grant. Authors thank Karen Arakelyan, Karen Avagyan,

[6] Calculations of the flux of runaway electrons produced by the lightning streamers suggests that stepped leaders produce a considerable number of energetic electrons, which is in an agreement with the number of energetic photons observed from satellites in terrestrial gamma ray flashes (Celectin and Pasko, 2011).

David Pokhsraryan, Arthur Reymers and David Sargsyan for assembling and launching Cube and STAND detectors. Authors are grateful to the members of the seminar of the cosmic ray division of Alikhanyan national lab for useful discussions and to S. Chilingaryan for developing ADEI multivariate visualization tool (Chilingaryan et al., 2010) for the treatment of the ASEC data flow. Gagik Hovsepyan helped in understanding asymmetries of the secondary cosmic ray flux and Laura Melkumyan made the histogram of the TGE events. Authors thank them for collaboration.

Appendix A. Disentangling of charged and neutral fluxes by ASEC detectors

The largest TGEs measured by the ASEC detectors originated from RREA process in thunderclouds located above Aragats research station. The electrons and gamma rays from the RREA are continuing their path in direction of the Earth after avalanche growth stopped reaching LPCR. Depending on the distance from LPCR to particle detectors the relative fraction of electrons to gamma rays is changing. Measured huge enhancement of count rates is due to electrons and gamma rays, because both neutral and charged particles can generate signals in plastic scintillators, although with different efficiencies. Therefore, to estimate energy spectra of electrons and gamma rays we need to disentangle the mixture of electrons and gamma rays. Special experimental facilities were designed and installed at Aragats for separating electron and gamma ray fluxes. Two 20 cm thick plastic scintillators located inside the Cube detector are completely surrounded by 1 cm thick molded plastic scintillators, which are shown in Fig. 13. Thick scintillators detect charged flux with very high efficiency (99%) and also neutral flux with efficiency of 20–30%. Thin scintillators also detect charged flux with very high efficiency (98–99%), though the efficiency of detecting neutral flux is highly suppressed and equals to 1–2%. Using advanced coincidence technique it is possible to purify the neutral flux detected by inside scintillators, rejecting the charged flux by signals from surrounding thin scintillators. The calibration of Cube detector proves that veto system (preventing counting signal in the thick scintillator if there is a signal in at least one of surrounding six thin scintillators) can reject 98% of the charged flux. Number of TGE particles detected by upper thick scintillator (detector surface 0.25 m^2, see Fig. 13) at 18:23, October 4, 2010 was $N(20\text{ cm}) = 43{,}439$ with veto and $N^v(20\text{ cm}) = 44{,}956$ without veto, the difference is $N - N^v = 1517$. By these counts we can recover the flux (number of particles per m^2 per minute) of electrons N_e and gamma rays N_g above the detector.

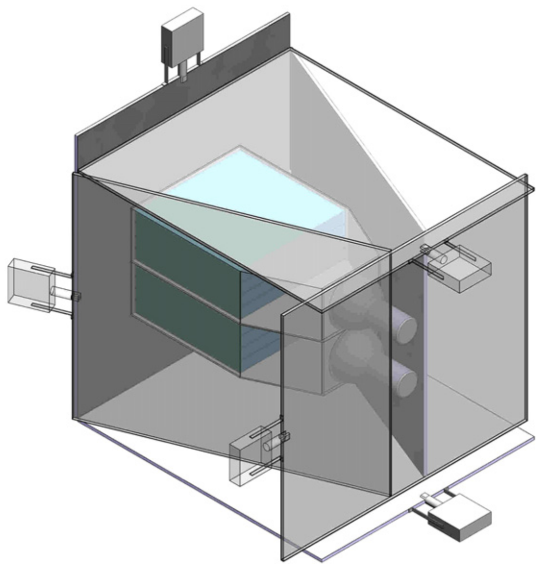

Fig. 13. Cube outdoor detector; thick scintillators located inside are measuring neutral flux with purity 98%.

$$\begin{aligned} N(20\,\text{cm}) &= N_e p(20\,\text{cm}/e) + N_g p(20\,\text{cm}/g) \\ N^v(20\,\text{cm}) &= N_e p^v(20\,\text{cm}/e) + N_g p^v(20\,\text{cm}/g), \end{aligned} \tag{1}$$

where p(20 cm/e) and p(20 cm/g) are the conditional probabilities to register electron or gamma ray by 20 cm scintillator. Accordingly p^v(20 cm/e) and p^v(20 cm/g) are the conditional probabilities to register electron or gamma ray by Cube 20 cm scintillator with veto switched on. By calibration, confirmed with detector response simulations, we estimate these conditional probabilities as follows:

$$\begin{aligned} &p(20\,\text{cm}/e) = .99 \\ &p(20\,\text{cm}/g) = 0.2 \\ &p(1\,\text{cm}/e) = 0.98 \\ &p(1\,\text{cm}/g) = 0.02 \\ &p^v(20\,\text{cm}/e) = (1-p(1\,\text{cm}/e))p(20\,\text{cm}/e) = (1\text{–}0.98)0.99 = 0.0198 \\ &p^v(20\,\text{cm}/g) = (1-p(1\,\text{cm}/g))p(20\,\text{cm}/g) = (1\text{–}0.02)0.2 = 0.196. \end{aligned} \tag{2}$$

Solving the system of Eq. (1) with coefficients (2) we readily get: $N_e = 1560$ and $N_g = 215{,}000$. Thus, on October 4, most of TGE particles were gamma rays, the fraction of electrons was less than 1%. From additional 1560 particles detected by 20 cm thick Cube scintillators only 31 can be electrons, i.e. less than 2%. Therefore, by examining the histograms of the energy deposits released in the thick scintillators of Cube we can recover the energy spectrum of the gamma rays of the TGE that happened on October 4, 2010 (see the techniques of the energy spectra recovering in the Appendix B). Of course, our calculations did not include the energy dependence of the efficiencies to detect gamma ray or electron by plastic scintillators; we assume that conditional probabilities are constant, according to Eq. (2). However, estimation of the energy dependence of these efficiencies by detector response function calculation with GEANT 4 code does not significantly alter our results. The ultimate check of the particle classification and energy spectra recovering will be an independent estimate of the particle enhancements registered with other ASEC detectors using those obtained by Cube energy spectra. The energy spectrum of gamma rays (Eq. (3)) obtained by the Cube detector was used to calculate the detector response of the STAND detector.

$$\begin{aligned} &dE/dN = 5.4e+07*\exp(-0.25*E) \\ &\quad \text{for the energy range of } 5\text{–}10\,\text{MeV}; \\ &dE/dN = 1.93e+08*E^{-3.3} \text{ for the energy range of } 10-50\,\text{MeV}; \end{aligned} \tag{3}$$

Another outdoor detector STAND, see Fig. 14, consists of three 1 cm thick scintillators of the same type as Cube veto scintillators. STAND detector DAQ electronics stored statistics of all possible coincidences of the 3 scintillator “firings”.

Denoting the scintillator, which detected a particle by “1” and the scintillator, which has not registered a particle by “0” we get 7 meaningful combinations (combination 000 has no sense). For instance, combination “100” corresponds to the case when low energy particle stops in the upper layer and does not reach the layers below; “111” combination corresponds to high-energy particle generating signal in all 3 scintillators.

In Table 1 we compare the measurement at 18:23 4 October 2010 coincidence statistics with simulated detector response on reconstructed by Cube gamma ray energy spectrum (3).

Rather good coincidence of the sum of the simulated electrons and gamma rays with measured particle confirms that used gamma ray energy spectrum (3) is valid. Furthermore, by the electron fraction of the total counts we can recover integral spectrum of the TGE electrons.

Table 1
Measured and simulated STAND statistics; 18:23, 4 October 2010.

	100	110	111
Experiment	95,025	7366	1836
Simulated gamma rays	62,832	3929	1377
Simulated electrons	32,193	3437	459

Appendix B. The method of TGE gamma ray and electron spectra recovery

The data acquisition (DAQ) electronics of the ASNT and Cube detectors stores each minute energy deposit histograms, digitized by Amplitude to digital converter (ADC) output analog signals of the photomultipliers (PM) overviewed the 60 cm and 20 cm thick scintillators located in the lightproof housings. On the basis of these histograms, using Monte Carlo techniques we recover differential energy spectra of the gamma rays. We solve the inverse problem and “unfold” the gamma-ray spectra by multiple solutions of the direct problem and comparisons of simulated and measured energy deposit histograms. Assuming the analytic form of the RREA gamma-ray spectra (power, exponential, or power with exponential cutoff) we tune free parameters (number of gamma-rays fallen on the roof and spectral indices) by minimizing the “quality” function describing the closeness of simulated with GEANT4 energy deposit histogram with the experimentally measured one. Gamma rays were traced through the material of the roof above the detector and trough the detector itself. The following steps were performed for the unfolding of the ASNT gamma ray spectrum above the roof of the MAKET building at an altitude of 3200 m:

- An energy spectrum with initial parameters randomly chosen from predetermined interval is generated;
- This spectrum is used to simulate the traversal of gamma rays through roof and ASNT detector components to finally obtain the energy deposit in thick scintillator;
- The obtained histogram of simulated energy deposits is compared with experimental one; the discrepancy (quality function) and initial spectrum parameters are stored;
- The simulations are continued till obtaining the histograms of energy releases corresponding to the whole interval of chosen spectrum parameters.

Having the dependence of the quality function on the test gamma ray spectra parameters, we fit these data by a second order polynomial function and find the minimum corresponding to the test gamma-ray spectrum, which generates an energy deposit spectrum closest to the experimentally measured one. For estimating the bias and accuracy of the above formulated procedure we simulate 150,000 gamma rays with energies distributed by power law with chosen spectral index equal to 3, i.e., $f(E)\sim E^{-3}$. Each gamma ray was followed by GEANT4 code, traversing the roof and detectors, and energy deposit in the scintillators was enumerated and stored. The obtained energy deposit histogram was taken as an “experimental” one and was further used for the energy spectrum recovery procedure. The gamma-ray spectra with power indices from -2 to -4 with step -0.01 were generated and corresponding energy deposit histograms were

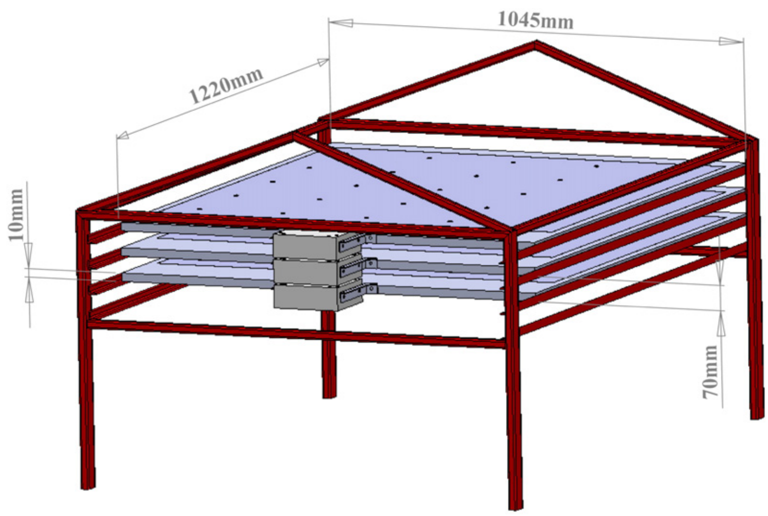

Fig. 14. STAND detector consisting of three layers of 1 cm thick scintillators.

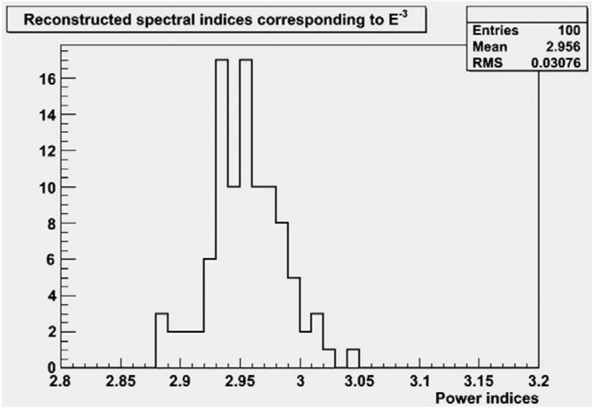

Fig. 15. Test of the spectral index recovery using a simulated spectrum as f(E) ~ E^{-3}.

generated. Quality functions between “measured” and simulated spectra were calculated; the value of power index corresponding to the minimum of the quality function was obtained. We have repeated this procedure with hundred independent random samples, which serve as experimental ones and for each of hundred we repeated the spectra recovery procedure. As we can see from the legend of Fig. 15 the negative bias of the method is 0.044 and RMS is ~0.031. The corresponding relative error of the power index estimate is ~2%, which is 3 times less than the statistical error.

The test spectra for the recovering of the gamma ray spectrum of October 4, 2010 TGE were simulated according to power law with spectral indices varying in the range of −2 to −4 with step 0.01. Simultaneously, both spectra measured by top and bottom 20 cm thick Cube scintillators were simulated. Two hundred trials were performed and quality functions were calculated each time to describe the closeness of the energy deposit obtained in simulation with the experimental one. In Fig. 16, the dependence of the quality function on spectral index is shown for upper and lower Cube scintillators. For the quality function the χ^2/ndf was chosen. The power spectra were found to give closer results to the

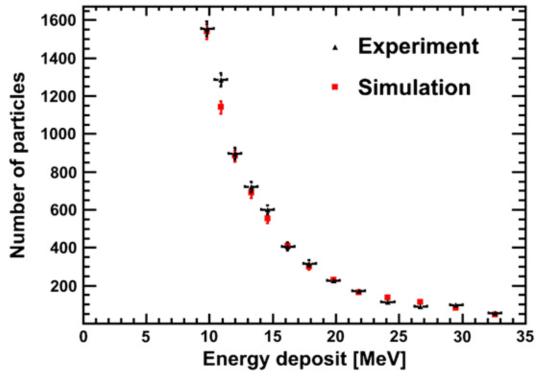

Fig. 17. Measured and simulated energy deposit histograms of Cube upper scintillator.

experiment. The values of the quality functions corresponding to the different indices of the power function are approximated by the second order polynomial and as the final estimate the power index corresponding to the minimum of the curve was chosen (see Fig. 16). The χ^2/ndf for the best-fit parameters is less than 1.

The obtained gamma-ray spectra by both Cube 20 cm detectors are in very good agreement with each other. The estimated gamma-ray spectrum by Cube upper scintillator for October 4, 2010 TGE is ~$E^{-3.3\pm0.2}$in the energy range >10 MeV; the gamma ray flux is ~150,000 particles/m^2/min at 18:23 UT on 4 October, 2010, at altitude of 3200 m above sea level. The recovered spectrum by Cube lower scintillator is ~$E^{-3.3\pm0.2}$. The October 4, 2010 TGE gamma-ray spectrum at energies 5–10 MeV is flatter and can be better described by the exponential function with index ~−0.25, the intensity is equal to ~400,000 particles/m^2/min. The “theoretical” (obtained by simulation, assuming power law spectrum of gamma rays above the outdoor Cube detector) and the measured energy deposit histograms of upper Cube scintillator are shown in Fig. 17.

However, the high-energy gamma rays will deposit small fraction of its energy in 20-cm thick scintillator and it will lead to possible biases in the high-energy spectra recovering.

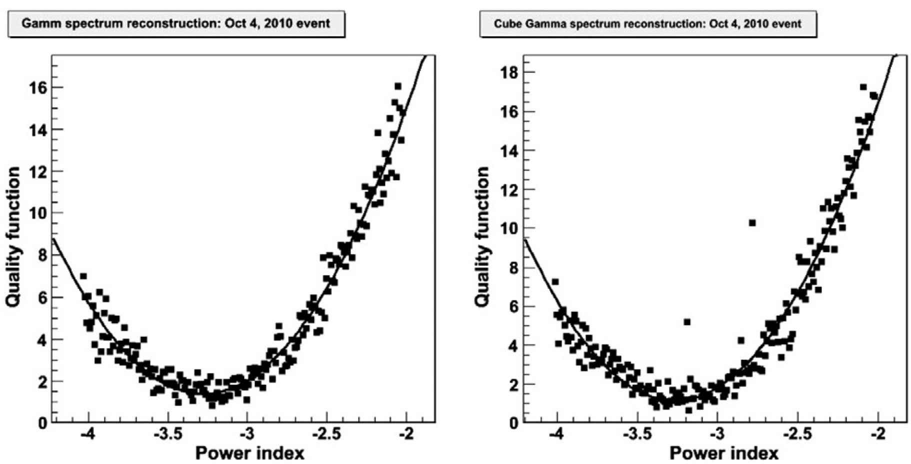

Fig. 16. The 200 trial spectra fitted by the second order polynomial (2 cube detectors data on 4 October, 2010).

As we are interested in proving the existence of high-energy tail, for gamma ray spectra recovering above 10 MeV we use 60 cm thick ASNT scintillators, more sensitive for high energies. The energy deposit histogram measured by one of the four ASNT scintillators with the best performance at low threshold (calibrated with spectra measured by Cube detector) was used for energy spectra recovering in high-energy domain. The gamma ray differential energy spectra above detector were estimated by multiple tests of propagation of the trial spectra through detector using GEANT4 code. Simulations in the energy range above 10 MeV were performed with power-law spectra in 2 versions: with maximal gamma-ray energy equal to 50 MeV and 100 MeV. In Fig. 18, the simulated energy deposit spectra obtained with assuming 50 MeV and 100 MeV along with the measured one are presented. The higher value of gamma ray maximal energy made the simulated spectrum closer to the experimental one. The error bars include the uncertainty in determination of the light attenuation coefficients in thick scintillator of ASNT detector. The quality function (χ^2/ndf) describing the closeness of simulated and measured histograms has a smaller value in case of 100 MeV maximal energy of incident gamma rays — ~3 instead of ~250 for 50 MeV.

Large values of χ^2/ndf reflect both possible errors in the used light attenuation coefficients and 2 modes of TGE origin. The fast decrease of experimental energy deposit spectrum at 17 MeV maybe is the illustration of the mode change of the TGE particle initiation.

The recovered gamma ray energy spectrum was checked by SEVAN detector, which can also distinguish neutral and charged fluxes. SEVAN DAQ electronics stores all possible combinations of signals (denoted by 1), and absence of signal (denoted by 0) in 3 layers. Combination "100" selects the low energy charged particles; coincidence "010" selects neutral particles, and combination "111" selects high-energy muons (see details in Chilingarian and Reymers, 2008). Simulating the passage of the recovered gamma-ray flux through the roof above and detector and taking into account the detector response to gamma rays and electrons, we have estimated the expected number of gamma rays detected by the "010" combination to be 1459 respectively. This value is in good agreement with experimentally measured value of 1452 ± 42.

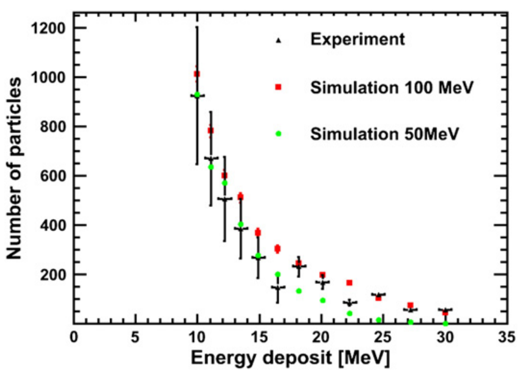

Fig. 18. Simulated and measured energy deposit spectra in the 60 cm thick scintillator of ASNT detector. Test power law spectra above detector were simulated in 2 versions: with maximal energy of 50 and 100 MeV.

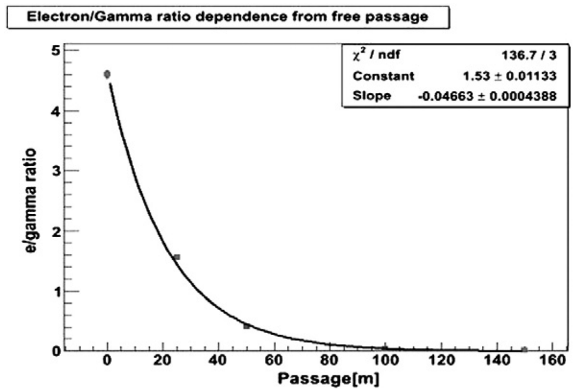

Fig. 19. Dependence of the electron/gamma ray ratio on the free passage distance after quitting the electrical field region.

Appendix C. Thundercloud height estimation; electron number estimation

From the estimated integral energy spectra of electrons and gamma rays of October 4, 2010, we can estimate the approximate altitude of the thundercloud (the altitude from where the electron flux is not accelerated anymore, but only attenuated). This distance can be estimated by the dependence of the electron/gamma ray ratio on these particles' passage in the atmosphere obtained by the simulations of the RREA process followed by the passage of particles in the air. Using the GEANT 4 code we simulate the electron-gamma ray avalanche in an electric field of 1.8 kV/cm prolonged 1.6 km and then — obtain the electron/gamma ray ratio for various passage distances. In Fig. 19, the electron/gamma ray ratio dependence on the passage distance is presented for particles with energies greater than 7 MeV.

From Fig. 20, where we presented integral energy spectra of electrons and gamma rays with energies higher than 1 MeV, along with cosmic ray background electrons and gamma rays at 3200 m, we readily get the electron/gamma ray ratio of 0.0135 for 7 MeV particles. From Fig. 18, we find that the passage distance value corresponding to the observed electron/gamma ray ratio equals ~130 m. The maximal energy of the detected electrons on October 4 was 12–14 MeV, therefore we

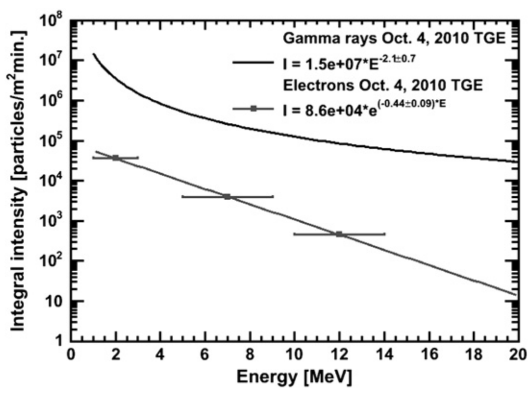

Fig. 20. Electron and gamma ray integral energy spectra of 4 October 2010 TGE as measured on 3200 m.

can estimate the maximal energy of the RREA electrons to be 30–40 MeV.

References

Aglietta, M., et al., EAS-TOP Collaboration, 1989. The EAS-TOP array at E0 = 1014–1016 eV: stability and resolutions. Nucl. Instrum. Methods Phys. Res., Sect. A 277, 23–28.

Agnsotelli, S., Allison, J., Amako, K., et al., 2003. GEANT4—a simulation toolkit. Nucl. Instrum. Methods Phys. Res., Sect. A 506, 250–303.

Alexeenko, V.V., Khaerdinov, N.S., Lidvansky, A.S., Petkov, V.B., 2002. Transient variations of secondary cosmic rays due to atmospheric electric field and evidence for pre-lightning particle acceleration. Phys. Lett. A 301, 299–306, http://dx.doi.org/10.1016/S0375-9601(02)00981-7.

Babich, L.P., Bochkov, L.I., Kutsyk, I.M., Roussel-Dupre, R.A., 2010. Localization of the source of terrestrial neutron bursts detected in thunderstorm atmosphere. J. Geophys. Res. 115, A00E28.

Babich, L.P., Bochkov, E.I., Kutzyk, I.M., 2011. Lightning initiation mechanism based on the development of relativistic runaway electron avalanches triggered by background cosmic radiation: numerical simulation. Russ. J. JETF 139, 1028–1036.

Briggs, M.S., Fishman, G.J., Connaughton, V., et al., 2011. Electron-positron beams from terrestrial lightning observed with Fermi GBM. Geophys. Res. Lett. 38, L02808.

Carlson, B.E., Lehtinen, N.G., Inan, U.S., 2008. Constraints on terrestrial gamma ray flash production from satellite observation. J. Geophys. Res. Lett. 34, L08809.

Carlson, B.E., Lehtinen, N.G., Inan, U.S., 2009. Terrestrial gamma ray flash production by lightning current pulses. J. Geophys. Res. 114, A00E08, http://dx.doi.org/10.1029/2009JA014531.

Celectin, S., Pasko, V.P., 2011. Energy and fluxes of thermal runaway electrons produced by exponential growth of streamers during the stepping of lightning leaders and in transient luminous events. J. Geophys. Res. 116 (A03315), 14, http://dx.doi.org/10.1029/2010JA016260.

Chilingarian, A., Reymers, A., 2008. Investigations of the response of hybrid particle detectors for the Space Environmental Viewing and Analysis Network (SEVAN). Ann. Geophys. 26, 249–257.

Chilingarian, A., Avagyan, K., Babayan, V., et al., 2003. Aragats Space-Environmental Center: status and SEP forecasting possibilities. J. Phys. G: Nucl. Part. Phys. 29, 939–952.

Chilingarian, A., Arakelyan, K., Avakyan, K., et al., 2005. Correlated measurements of secondary cosmic ray fluxes by the Aragats Space-Environmental Center monitors. Nucl. Instrum. Methods Phys. Res., Sect. A 543 (2–3), 483–496.

Chilingarian, A., Daryan, A., Arakelyan, K., et al., 2010. Ground-based observations of thunderstorm-correlated fluxes of high-energy electrons, gamma rays, and neutrons. Phys. Rev. D 82, 043009.

Chilingarian, A., Hovsepyan, G., Hovhannisyan, A., 2011. Particle bursts from thunderclouds: natural particle accelerators above our heads. Phys. Rev. D 83, 062001.

Chilingaryan, S., Chilingarian, A., Danielyan, V., Eppler, W., 2008. The Aragats data acquisition system for highly distributed particle detecting networks. J. Phys. Conf. Ser. 119, 082001.

Chilingaryan, S., Beglarian, A., Kopmann, A., Voekling, S., 2010. Advanced data extraction infrastructure: web based system for management of time series data. J. Phys. Conf. Ser. 219, 042034.

Cui, H., Qie, X., Zhang, Q., Zhang, T., Zhang, G., Yang, J., 2009. Intracloud discharge and the correlated basic charge structure of a thunderstorm in Zhongchuan, a Chinese Inland Plateau region. Atmos. Res. 91, 425–429.

Cummer, S.A., Zhai, Y., Hu, W., Smith, D.M., Lopez, L.I., Stanley, M.A., 2005. Measurements and implications of the relationship between lightning and terrestrial gamma ray flashes. Geophys. Res. Lett. 32, L08811, http://dx.doi.org/10.1029/2005GL022778.

Cummer, S.A., Lu, G., Briggs, M.S., Connaughton, V., Xiong, S., Fishman, G.J., Dwyer, J.R., 2011. The lightning–TGF relationship on microsecond timescales. Geophys. Res. Lett. 38, L14810, http://dx.doi.org/10.1029/2011GL048099.

De Souza, P.E., Pinto Jr., O., Pinto, I.R.C.A., Ferreira, N.J., Dos Santos, A.F., 2009. The intracloud/cloud-to-ground lightning ratio in Southeastern Brazil. Atmos. Res. 91, 491–499, http://dx.doi.org/10.1016/j.atmosres.2008.06.011.

Dorman, L.I., Dorman, I.V., 2005. Possible influence of cosmic rays on climate through thunderstorm clouds. Adv. Space Res. 35, 476–483.

Dwyer, J.R., 2003. A fundamental limit on electric fields in air. Geophys. Res. Lett. 30, 2055.

Dwyer, J.R., 2004. Implications of X-ray emission from lightning. Geophys. Res. Lett. 31, L12102, http://dx.doi.org/10.1029/2004GL019795.

Dwyer, J.R., 2005. The initiation of lightning by runaway air breakdown. Geophys. Res. Lett. 32, L20808.

Dwyer, J.R., 2007. Relativistic breakdown in planetary atmospheres. Phys. Plasmas 14, 042901.

Dwyer, J.R., 2012. The relativistic feedback discharge model of terrestrial gamma ray flashes. J. Geophys. Res. 117, A02308, http://dx.doi.org/10.1029/2011JA017160.

Dwyer, J.R., Smith, D.M., 2005. A comparison between Monte Carlo simulations of runaway breakdown and terrestrial gamma-ray flash observations. Geophys. Res. Lett. 32, L08811.

Fishman, G., Bhat, P.N., Malozzi, R., et al., 1994. Discovery of intense gamma-ray flashes of atmospheric origin. Science 264, 1313–1316.

Gurevich, A.V., Milikh, G.M., Roussel-Dupre, R., 1992. Runaway electron mechanism of air breakdown and preconditioning during a thunderstorm. Phys. Lett. A 165, 463–468.

Gurevich, A., Zybin, K., Roussel-Dupre, R., 1999. Lightning initiation by simultaneous effect of runaway breakdown and cosmic ray showers. Phys. Lett. A 254, 79–87.

Gurevich, A.V., Mitko, G., Antonova, V., et al., 2009. An intracloud discharge caused by extensive atmospheric shower. Phys. Lett. A 373 (39), 3550–3553.

Khaerdinov, N.S., Lidvansky, A.S., Petkov, V.B., 2005. Cosmic rays and the electric field of thunderclouds: evidence for acceleration of particles (runaway electrons). Atmos. Res. 76, 346–354.

Lehtinen, N.G., Bell, T.F., Inan, U.S., 1999. Monte Carlo simulation of runaway MeV electron breakdown with application to red sprites and terrestrial gamma ray flashes. J. Geophys. Res. 104 (A11), 24,699–24,712.

Lidvansky, A.S., Khaerdinov, N.S., 2009. Strong variations of cosmic ray muons during thunderstorms. Izv. Ross. Akad. Nauk, Ser. Fiz. 73, 415–417 [Bulletin of the Russian Academy of Sciences: Physics 73, 400 (2009)]..

Lu, G., Blakeslee, R.J., Li, J., Smith, D.M., Shao, X.-M., McCaul, E.W., Buechler, D.E., Christian, H.J., Hall, J.M., Cummer, S.A., 2010. Lightning mapping observation of a terrestrial gamma-ray flash. Geophys. Res. Lett. 37, L11806, http://dx.doi.org/10.1029/2010GL043494.

Lu, G., Cummer, S.A., Li, J., Han, F., Smith, D.M., Grefenstette, B.W., 2011. Characteristics of broadband lightning emissions associated with terrestrial gamma ray flashes. J. Geophys. Res. 116, A03316, http://dx.doi.org/10.1029/2010JA016141.

Moss, G.D., Pasko, V.P., Liu, N., Veronis, G., 2006. Monte Carlo model for analysis of thermal runaway electrons in streamer tips in transient luminous events and streamer zones of lightning leaders. J. Geophys. Res. 111, A02307, http://dx.doi.org/10.1029/2005JA011350.

Muraki, Y., Axford, W.I., Matsubara, Y., et al., 2004. Effects of atmospheric electric fields on cosmic rays. Phys. Rev. D 69, 123010.

Nag, A., Rakov, V.A., 2009. Some inferences on the role of lower positive charge region in facilitating different types of lightning. Geophys. Res. Lett. 36, L05815, http://dx.doi.org/10.1029/2008GL036783.

Pawar, S.D., Kamra, A.K., 2004. Evolution of lightning and the possible initiation/triggering of lightning discharges by the lower positive charge center in an isolated thundercloud in the tropics. J. Geophys. Res. 109, D02205.

Pinto Jr., O., Pinto, I.R.C.A., Naccarato, K.P., 2007. Maximum cloud-to-ground lightning flash densities observed by lightning location systems in the tropical region: a review. Atmos. Res. 84, 189–200.

Qie, X., Zhang, T., Chen, C., Zhang, G., Zhang, T., Kong, X., 2009. Electrical characteristics of thunderstorms in different plateau regions of China. Atmos. Res. 91, 244–249.

Sato, T., Endo, A., Zanki, M., Petoussi-Henss, N., Niita, K., 2009. Fluence-to-dose conversion coefficients for neutrons and protons calculated using the PHITS code and ICRP/ICRU adult reference computational phantoms. Phys. Med. Biol. 54, 1997.

Schonland, B.F.J., 1930. Thunder-storms and the penetrating radiation. Proc. R. Soc. Lond. A 130, 37.

Schonland, B.F.J., Viljoen, J.P.T., 1933. On a penetrating radiation from thunderclouds. Proc. R. Soc. Lond. A 140, 314.

Shao, X.M., Hamlin, T., Smith, D., 2010. A closer examination of terrestrial gamma-ray flash-related lightning processes. J. Geophys. Res. 115, A00E30, http://dx.doi.org/10.1029/2009JA014835.

Shaw, G.E.J., 1967. Cosmic count increase associated with thunderstorms. Geophys. Res. Bull. 72, 4623.

Standler, R.B., Winn, W.P., 1979. Effects of coronae on electric field beneath thunderstorms. Quart. J. Roy. Meteor. Soc. 105, 285–302.

Stanley, M., Shao, X.M., Smith, D., et al., 2006. A link between terrestrial gamma-ray flashes and intracloud lightning discharges. Geophys. Res. Lett. 33, L06803, http://dx.doi.org/10.1029/2005GL025537.

Stolzenburg, M., Marshall, T.C., Rust, W.D., 1998. Electrical structure in thunderstorm convective regions 2. Isolated storms. J. Geophys. Res. 103, 14079.

Torii, T., Takeishi, M., Hosono, T., 2002. Observation of gamma-ray dose increase associated with winter thunderstorm and lightning activity. J. Geophys. Res. 107, 4324, http://dx.doi.org/10.1029/2001JD000938.

Torii, T., Sugita, T., Tanabe, S., Kimura, Y., Kamogawa, M., Yajima, K., Yasuda, H., 2009. Gradual increase of energetic radiation associated with

thunderstorm activity at the top of Mt. Fuji. Geophys. Res. Lett. 36, L13804, http://dx.doi.org/10.1029/2008GL037105.
Torii, T., Sugita, T., Kamogawa, M., et al., 2011. Migrating source of energetic radiation generated by thunderstorm activity. Geophys. Res. Lett. 38, L24801, http://dx.doi.org/10.1029/2011GL049731.
Tsuchiya, H., Enoto, T., Yamada, S., et al., 2007. Detection of high-energy gamma rays from winter thunderclouds. Phys. Rev. Lett. 99, 165002.
Tsuchiya, H., Enoto, T., Torii, T., et al., 2009. Observation of an energetic radiation burst from mountain-top thunderclouds. Phys. Rev. Lett. 102, 255003.
Tsuchiya, H., Enoto, T., Yamada, S., et al., 2011. Long-duration gamma ray emissions from 2007 and 2008 winter thunderstorms. J. Geophys. Res. 116, D09113, http://dx.doi.org/10.1029/2010JD015161.
Vernetto, S., for EAS-TOP Collaboration, 2001. The EAS counting rate during thunderstorms. Proceedings of the 27th International Cosmic Ray Conference (ICRC) (Copernicus Gesellschaft, Hamburg, Germany, 2001), 10, pp. 4165–4168.
Wentz, J., Brancus, I.M., Bercuci, A., Heck, D., Oehlschlager, J., Rebel, H., Vulpescu, B., 2003. Simulation of atmospheric muon and neutrino fluxes with CORSIKA. Phys. Rev. D 67, 073020.
Williams, E.R., 1989. The tripole structure of thunderstorms. J. Geophys. Res. 94, 13151–13167.
Wilson, C.T.R., 1925. The acceleration of b-particles in strong electric fields such as those of thunderclouds. Proc. Camb. Philos. Soc. 22, 534–538, http://dx.doi.org/10.1017/S0305004100003236.